

Self-Assembled Organic Nanostructures: Effect of Substituents on the Morphology**

Wei Su, Yuexing Zhang, Chuntao Zhao, Xiyou Li,* and Jianzhuang Jiang*[a]

Three perylene-3,4,9,10-tetracarboxydiimide (PTCDI) compounds with two dodecyloxy or thiododecyl chains attached at the bay positions of the perylene ring, PTCDIs 1–3, were fabricated into nanoassemblies by a solution injection method. The morphologies of these self-assembled nanostructures were determined by transmission electronic microscopy (TEM), scanning electronic microscopy (SEM), and atomic force microscopy (AFM). PTCDI compound 1, with two dodecyloxy groups, forms long, flexible nanowires with an aspect ratio of over 200, while analogue 3, with two thiododecyl groups, self-assembles into spherical particles. In line with these results, PTCDI 2, with one dodecyloxy group and one thiododecyl group, forms nanorods with an aspect ratio of around 20. Electronic absorption and fluorescence spectroscopy

results reveal the formation of H-aggregates in the nanostructures of these PTCDI compounds owing to the π - π interaction between the substituted perylene molecules and also suggest a decreasing π - π interaction in the order 1 > 2 > 3, which corresponds well with the morphology of the corresponding nanoassemblies. On the basis of DFT calculations, the effect of different substituents at the bay positions of the perylene ring on the π - π interaction between substituted perylene molecules and the morphology of self-assembled nanostructures is rationalized by the differing degree of twisting of the conjugated perylene system caused by the different substituents and the different bending of the alkoxy and thioalkyl groups with respect to the plane of the naphthalene.

Introduction

Organic nanoassemblies are important building blocks for higher-order architectures. These nanostructures, in particular those constructed from functional organic molecules, are expected to be of use in a wide range of applications in nanoscience and nanotechnology as advanced materials for photovoltaic cells,^[1] light-emitting diodes (LEDs),^[2] and optical sensors.^[3] The construction of organic nanostructures through self-assembly of organic molecules driven by supramolecular interactions has been the focus of much research interest over the past decade. Intensive studies have led to reports of various kinds of self-assembled organic nanostructures with different morphologies, including nanowires,^[4,5] nanorods,^[6] nanoparticles,^[7] and nanotubes.^[8] However, the construction of organic nanoassemblies into a particular structure with a controlled morphology depends on modification of the molecular structure and on tuning the supramolecular interaction, and it still remains a challenge for chemists and material scientists.

As an important functional dye with outstanding photostability and chemical stability, perylene-3,4,9,10-tetracarboxydiimide (PTCDI) derivatives have been intensively studied for several decades.^[9–12] In recent years, great efforts have been made to fabricate PTCDIs into nanostructures with various morphologies because of their potential applications in molecular electronics.^[13–21] Studies have revealed that the self-assembly of PTCDI molecules is dominated by π - π interactions between the conjugated perylene systems along with hydrogen bonding and liquid-crystal interactions.^[22–24] By introducing different side chains onto the imide nitrogen atoms of the perylene backbone to tune the π - π interactions between perylene systems, PTCDI nanoassemblies with various structures and mor-

phologies have been prepared by Zang and co-workers.^[25,26] Meijer and co-workers have also prepared chiral PTCDI nanofibers by incorporating two chiral oligo(*p*-phenylene vinylene) (OPV) groups at the imide nitrogen atoms of the perylene ring.^[27] Würthner and co-workers have reported the self-assembled supramolecular structure of OPV-PTCDI-OPV and OPV-PTCDI systems in methylcyclohexane (MCH), which is driven by the hydrogen-bonding and liquid-crystal-forming properties of the molecules, and characterized the products only on the basis of UV/Vis spectroscopy and molecular modeling.^[28,29] Recently, the same group reported the effect of halogen atoms at the bay positions of the perylene ring on the structure and morphology of the corresponding PTCDI nanoassemblies.^[18] They have also studied the self-assembly properties of PTCDI with tridodecylphenyl substituents at the imide positions.^[20] The hydrophobic interaction between these tridodecylphenyl groups was found to dominate the process of self-assembly and to bring about the molecules' liquid-crystal properties. However, to our knowledge, the effect of alkoxy and thioalkyl groups (in particular, the effect of atoms linking the alkyl side

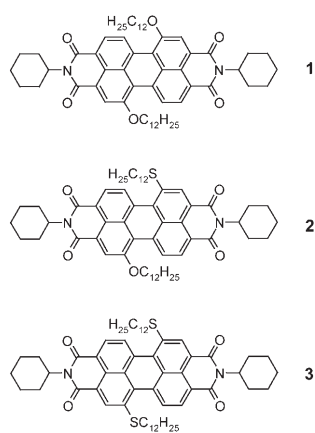
[a] W. Su, Y. Zhang, C. Zhao, Prof. X. Li, Prof. J. Jiang
Department of Chemistry, Shandong University
Jinan 250100 (China)
Fax: (+86) 531-856-5211
E-mail: jzjiang@sdu.edu.cn
xiyouli@sdu.edu.cn

***] Perylene-3,4,9,10-Tetracarboxydiimides with Two Dodecyloxy or Thiododecyl Groups at the Bay Positions

Supporting information for this article is available on the WWW under <http://www.chemphyschem.org> or from the author.

chains to the perylene ring) on the structure and morphology of self-assembling PTCDI nanostructures is still unknown.

To obtain more information about the relationship between the molecular structure and the corresponding organic nano-assembly and to control the structure and morphology of the nanoassembly of organic functional materials through molecular design, we describe herein the structure and morphology of three PTCDI nanoassemblies prepared from PTCDI compounds with different substituents at the bay positions of the perylene ring: *N,N'*-dicyclohexyl-1,7-di(dodecyloxy)-perylene-3,4:9,10-tetracarboxydiimide (**1**), *N,N'*-dicyclohexyl-1-thiododecyl-7-dodecyloxy-perylene-3,4:9,10-tetracarboxydiimide (**2**), and *N,N'*-dicyclohexyl-1,7-di(thiododecyl)-perylene-3,4:9,10-tetracarboxydiimide (**3**). As shown in Scheme 1, two dodecyl chains



Scheme 1. Schematic molecular structures of PTCDI **1–3**.

were introduced onto the perylene ring while leaving the rest of the molecule remaining unchanged. The π - π interactions between the conjugated perylene systems is the driving force for the self-assembly of these PTCDI compounds, which provides an ideal model system to study the effect of linking atoms between long alkyl side chains and the perylene ring on the aggregation behavior of organic functional molecules.

Results and Discussion

Spectral Characterization in Solutions

Figure 1 shows the electronic absorption spectra of PTCDI **1–3** dissolved in chloroform and methanol. As shown in Figure 1A, the maximum absorption band of **1** experiences a significant blue shift from 572 nm in chloroform to 506 nm in methanol, indicating the formation of H-type PTCDI aggregates in methanol with a typical face-to-face configuration arising from the strong π - π interaction between conjugated perylene systems.^[30,31] A similar but smaller blue shift was also observed in the main absorption band of PTCDI **2** in methanol compared with that in chloroform, as shown in Figure 1B, revealing a weaker π - π interaction in the aggregates of PTCDI **2**

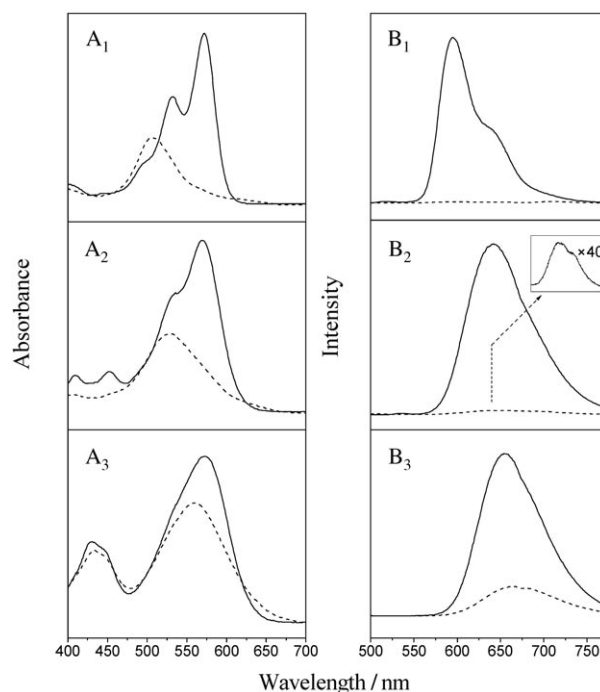


Figure 1. Electronic absorption (A) and fluorescence (B) spectra of PTCDI **1–3** (indicated by corresponding subscripts) in chloroform (—) and methanol (---). The inset of **B₂** shows the enlarged fluorescence spectrum of PTCDI **2**.

than **1**. The even smaller blue shift of the main electronic absorption band observed for PTCDI **3** in methanol versus in chloroform suggests that in methanol, **3** has the weakest π - π interactions between the perylene rings of the three systems studied. These electronic absorption spectroscopic results indicate that the three PTCDI derivatives **1–3** self-assemble into H-aggregates in methanol with the extent of π - π interactions between the PTCDI rings decreasing in the order **1** > **2** > **3**. This conclusion was additionally supported by their fluorescence behaviors in chloroform and methanol, see below.

The fluorescence spectra of PTCDI compounds **1–3** in chloroform and methanol are also compared in Figure 1. Fluorescence quantum yields (Φ_f) were measured with *N,N'*-dihexyl-1,7-di(4-*tert*-butylphenoxy)perylene-3,4:9,10-tetracarboxydiimide in chloroform as a standard ($\Phi_f = 100\%$) following the literature method.^[36] Fluorescence quantum yields for PTCDI compounds **1**, **2**, and **3** in methanol were calculated to be 0.7%, 1.6%, and 3.3%, respectively. This significant fluorescence quenching for these three PTCDI compounds in methanol compared with in chloroform might be ascribed to the formation of H-aggregates.^[32–35] The almost complete fluorescence quenching observed for PTCDI **1** and **2** in methanol indicates the formation of aggregates with very strong intermolecular π - π interactions between the perylene rings of these compounds. In contrast, the incomplete fluorescence quenching for PTCDI **3** in methanol obviously suggests the formation of relative unstable aggregates with weak π - π interactions. These results are further rationalized on the basis of theoretical calculation data as detailed below.

Aggregate Morphology

In line with the electronic absorption and fluorescence spectroscopic results, strong π - π interactions between perylene rings of PTCDI **1** are also verified by the formation of one-dimensional molecular stacks. Figure 2A shows a large-area transmis-

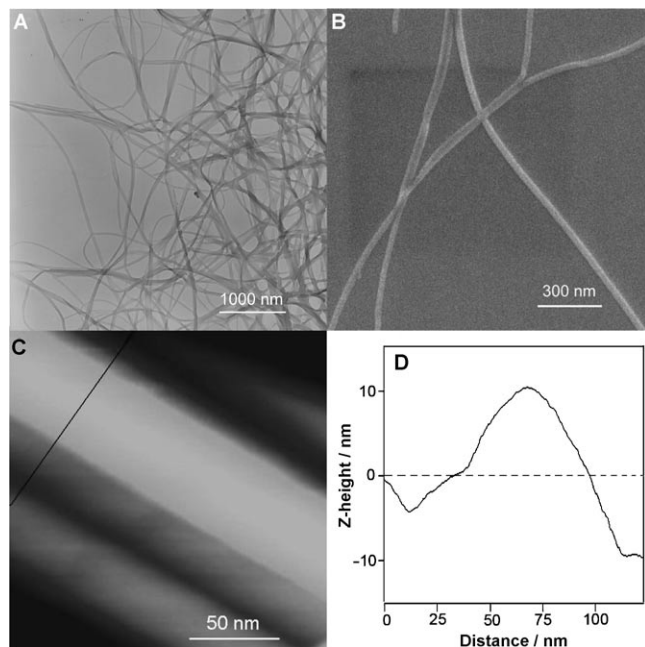


Figure 2. A) TEM image of PTCDI **1** nanowires cast on carbon film; B) SEM image of gold-stained nanowires cast on carbon film; C) A high-magnification AFM image of a single nanowire, and D) Z-height line-scan profile over the single wire marked by the black line in (C).

sion electron microscopy (TEM) image of nanostructures of PTCDI **1**. It can be seen that long, flexible nanowires with uniform width and length were formed in methanol. The columned-wire configuration of these nanostructures was also clearly shown in scanning electron microscopy (SEM) images of several nanowires (Figure 2B). The wire morphology was also revealed by atomic force microscopy (AFM) measurements (Figures 2C and D). It is worth noting that the diameter of the nanowires is about 20 nm, and their length is several micrometers, resulting in an aspect ratio (length over width) of over 200.

Similarly, the morphology of the nanoassemblies of PTCDI **2** and **3** was carefully characterized with a range of microscopic techniques. Figure 3 shows SEM images of the nanostructures of the three PTCDI compounds. Unlike the aggregates of PTCDI **1** with a long, flexible nanowire morphology, substitution of one of the two dodecyloxy chains in **1** by a thiododecyl group in **2** induces a significant change in the structure and morphology of the corresponding nanoassemblies formed under the same experimental conditions. With the decreased π - π interactions between the perylene rings of the molecules of compound **2**, which is due to the increased twisting of the perylene ring because of the change of one bridging atom be-

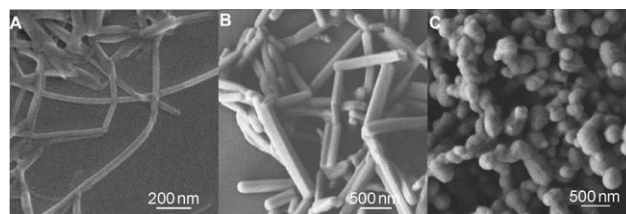


Figure 3. SEM images of the nanostructures of A) PTCDI **1**, B) PTCDI **2**, and C) PTCDI **3**.

tween the dodecyl and conjugated perylene system from a small oxygen atom to a large sulfur atom, short, rigid one-dimensional nanorods with a quadrilateral profiles instead of long, flexible nanowires are formed for PTCDI **2**. The rod morphology was also revealed by AFM and TEM measurements, (see Figure S1 in the Supporting Information). The wall thickness of the PTCDI **2** nanorods was found to be in the range 50–70 nm and their length was about 1 μ m, leading to an aspect ratio of about 15–20, which is obviously smaller than that of PTCDI **1**. More interestingly, further weakened π - π interactions between the perylene rings of PTCDI **3** molecules arising from the substitution of two dodecyloxy groups by two thiododecyl chains induced the formation of zero-dimensional particulate nanoaggregates. As shown in Figure 3C, the molecular assembly of PTCDI **3** is approximately spherical with an average diameter of about 100 nm, as shown by the TEM and AFM images (Figure S2 in the Supporting Information).

The structures of the nanoassemblies were further investigated by X-ray diffraction (XRD) techniques. Figure 4 shows the diffraction patterns of the three self-assembled nanostructures. All three nanoassemblies present large and relatively sharp diffraction peaks in the low-angle region, suggesting ordered molecular packing. The PTCDI **1** nanowires gave a diffraction peak at almost the same position as the PTCDI **2** nanorods, 4.64 and 4.51° for **1** and **2**, respectively, suggesting a similar microstructure in the nanoassemblies of these two compounds. The d spacing calculated according to these 2θ values is about 19.5 Å, which can be ascribed to the distance between the two cyclohexyl groups at the imide nitrogen atoms of the PTCDI molecules.^[35] These results suggest that the PTCDI molecules form H-aggregates in the nanoassembly and support the suggestion that PTCDI compounds **1** and **2** are predisposed to grow into one-dimensional aggregates (Figure 4A). The wide-angle region in the diffraction pattern of PTCDI derivatives **1** and **2** did not give any useful information. In contrast, the diffraction pattern for the self-assembled particulate nanoaggregates of PTCDI **3** showed strong peaks at $2\theta = 3.36^\circ$ (100), 6.74° (200), 9.25° (010), 10.57° (400), 18.71° (001), and 20.86° (110), which are reasonably assigned to a rectangular structure whose cell parameters are $a = 26.4$ Å, $b = 9.6$ Å, and $c = 4.7$ Å, with each cell consisting of two molecules of **3** (Figure 4B). Obviously, the configuration of the cell employed by the molecules of **3** limits the π - π interaction between neighboring cells and therefore prevents the aggregate from growing into long nanowires or nanorods.

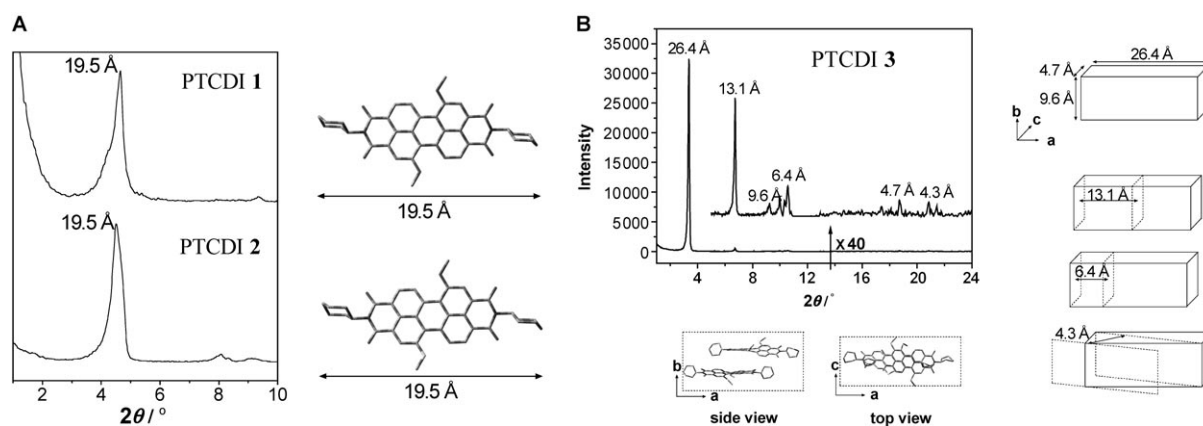


Figure 4. A) XRD profile of the aggregates of PTCDI 1 and 2. B) XRD profile and the schematic representation of the unit cell of the aggregates of PTCDI 3.

DFT Calculations

To enhance the understanding of the effect of substituents at the bay positions of the perylene rings on the self-assembly properties of PTCDI derivatives, density functional theory (DFT) calculations^[20,40] were carried out on the basis of simplified molecular models in which the alkoxy and thioalkyl substituents were replaced with methoxy and thiomethyl groups and the cyclohexyl groups linked at the two imide nitrogen positions were replaced by hydrogen atoms (Figure 5). The minimized structures of the three model compounds, including the schematic molecular structure diagram, molecular orbital map, and schematic one-dimensional stacking diagram, are shown in Figure 5. The result for the orbital map of PTCDI 1 (Figure 5B₁) indicates that the same orientation for the 2p_z orbitals of O₂₁ and C₁₇ leads to strong repulsion between these two orbitals, which induces a twisted configuration of the two naphthalene rings in the perylene ring, resulting in a distorted conjugated perylene system in the di(alkoxy)-substituted PTCDI 1. This is also true for the di(thioalkyl)-substituted PTCDI 3 as well as the mono(alkoxy)-mono(thioalkyl)-substituted PTCDI 2. These results clearly reveal that substitution of hydrogen atoms with either alkoxy or thioalkyl groups at the

bay positions of the perylene ring induces distortion of the conjugated perylene system in the PTCDI derivatives.

The atomic radius of the O atom is smaller than that of the S atom. Therefore, the repulsion between the 2p_z orbitals of O₂₁ and C₁₇ in PTCDI 1 is weaker than that between the 3p_z or-

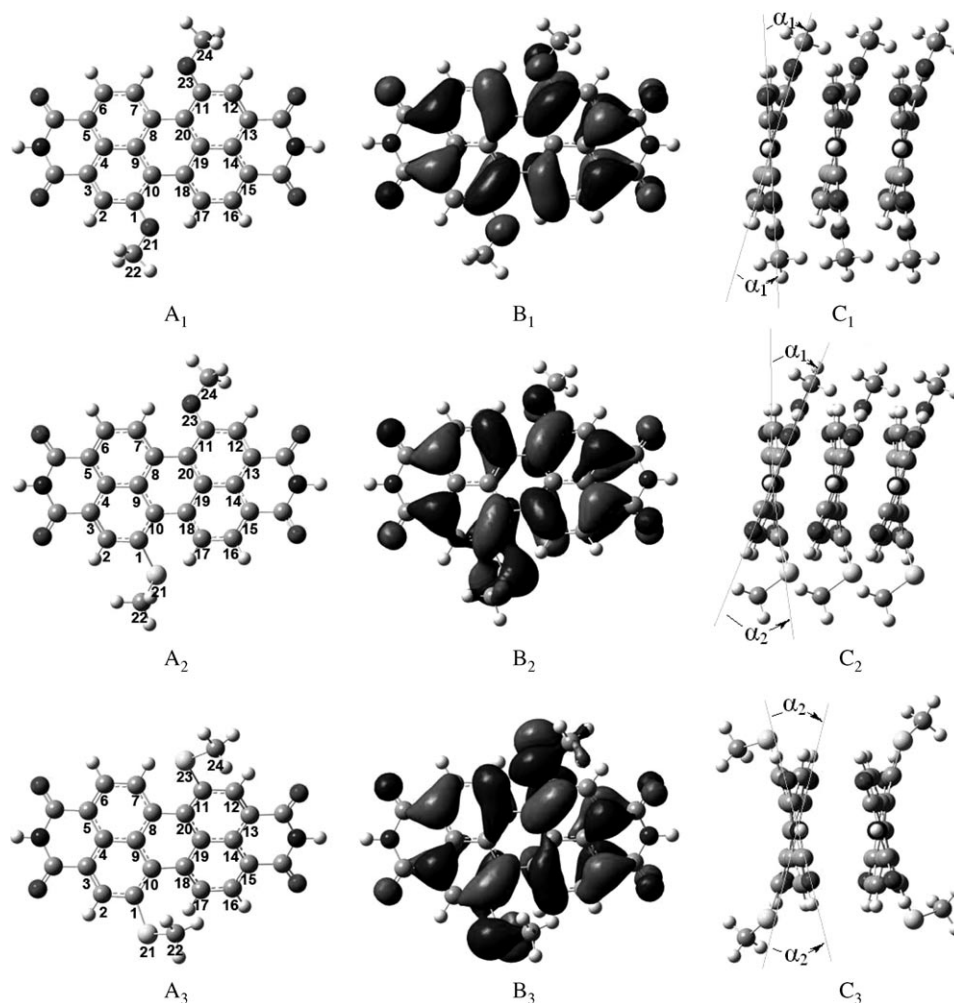


Figure 5. The energy-minimized configuration of predigested PTCDI 1–3. Schematic molecular structure diagram of structure (A), molecular orbital map (B), and schematic one-dimensional stacking diagram (C). Subscripts refer to the corresponding PTCDI compound.

bital of S_{21} and the $2p_z$ orbital of C_{17} in PTCDI **3**. This leads to a smaller degree of distortion of the perylene system in PTCDI **1** with a twisting angle between the two naphthalene rings of 15° (α_1) compared to 23° (α_2) in PTCDI **3** (Figure 5C). In line with the experimental findings, the smaller degree of distortion of the conjugated perylene system in PTCDI **1** does not significantly affect the π - π interaction between the molecules of PTCDI **1**, which self-assemble into one-dimensional nanowires because of the strong π - π interaction. In contrast, zero-dimensional particulate nanostructures are formed by PTCDI **3** because of the weakened π - π interaction between the molecules, which is associated with the large degree of distortion of the conjugated perylene system. As an intermediate compound between the di(alkoxy)-substituted PTCDI **1** and di(thioalkyl)-substituted PTCDI **3**, PTCDI **2** is substituted with one alkoxy chain and one thioalkyl group at each of the two bay positions of the perylene ring. It self-assembles into short, rigid one-dimensional nanorods with a quadrilateral profile.

On the basis of our calculations, the skeleton of the methoxy group is coplanar to the naphthalene ring to which it is attached in the alkoxy-substituted PTCDI compound (Figure 5). As a consequence, the methoxyl groups in the molecules of the corresponding PTCDI compound **1** give no steric hindrance to the self-assembly process in terms of spatial arrangement and therefore also contribute to the formation of one-dimensional long, flexible nanowires of PTCDI **1**. In contrast, the thiomethyl groups bend away from the plane of the naphthalene ring to which the thiomethyl group is attached in the thioalkyl-substituted PTCDI compound **3** (Figure 5), which results in steric hindrance to the face-to-face molecular packing of the corresponding compound and may therefore also be partially responsible for the failure of PTCDI **3** to form one-dimensional long nanostructures.

Conclusions

In summary, we have investigated the morphology and structures of the self-assembly of three PTCDI derivatives substituted with different side chains at the bay positions of the perylene ring. The PTCDI compound with two dodecyloxy substituent groups (**1**) self-assembled into one-dimensional nanowires owing to the strong π - π interaction between the PTCDI units. Substitution of the two dodecyloxy groups by two thiododecyl groups (compound **3**) induced a large torsion on the conjugated perylene system, which diminished the π - π interaction between the substituted perylene molecules, therefore resulting in the formation of zero-dimensional nanoassemblies. An intermediate perylene compound with one dodecyloxy and one thiododecyl group (**2**) forms one-dimensional nanorods with a morphology lying between those of the other two compounds. The effect of different side chains at the bay positions on the assembly properties of the substituted perylene compounds was reproduced by molecular structure calculations based on DFT. We believe that these results will be helpful in guiding the fabrication of organic functional materials into nanostructures for molecular electronic devices using molecular design and synthesis.

Experimental Section

The PTCDI compounds **1–3** were synthesized and purified according to the published procedure.^[36] The compounds were characterized by ^1H NMR spectroscopy (600 MHz) and shown to be free of 1,6 isomers. Both chloroform and methanol (HPLC grade) were purchased from Tianjin Kernel Co. The nanostructures of the three compounds were fabricated by the re-precipitation method according to the following procedure:^[25,26,37–39] A minimum volume (5–125 μL) of concentrated chloroform solution of PTCDI (1 mM) was injected rapidly into a larger volume of methanol (2.5 mL) and subsequently mixed with a microinjector. The nanoparticles of the PTCDI compounds were then separated from the solvents immediately. The experiments were carried out on PTCDI solutions at different concentrations and at different injection speeds at room temperature. The results were stable and reproducible under the experimental conditions described above.

Electronic absorption and fluorescence spectra were recorded on a Shimadzu UV-1650PC spectrometer and a K2 system (ISS), respectively. Low-angle X-ray diffraction (XRD) measurements were carried out on a Rigaku D/max- ζB X-ray diffractometer. TEM images were taken on a JEOL JEM-100CX II electron microscope operated at 100 kV. SEM images were obtained using a JEOL JSM-6700F field-emission scanning electron microscopy. AFM images were collected in air under ambient conditions using the tapping mode with a Nanoscope III/Bioscope scanning probe microscope from Digital Instruments. For TEM imaging, the sample of PTCDI nanoparticles in methanol was cast onto a TEM grid (Cu with a carbon film). For SEM imaging, Au (1–2 nm) was sputtered onto these grids to prevent charging effects and to improve image clarity. For AFM imaging, the sample was cast onto a SiO_2 surface.

The frontier molecular orbital calculations for the three PTCDI derivatives were carried out using DFT. The hybrid density functional B3LYP (Becke-Lee-Young-Parr composite exchange–correlation functional) was used for both geometry optimizations and property calculations. In all cases, the 6-31G (d) basis set was used. The Berny algorithm using redundant internal coordinates was employed for the energy minimization and the default cutoffs were used throughout.^[40] Using the energy-minimized structures, normal coordinate analyses were carried out. To verify that these energy-minimized structures are true energy minimums, vibration frequency calculations were performed. The fact that no imaginary vibration was predicted in the frequency calculations confirms that the energy-minimized structures for all three compounds are true energy minimums. All calculations were carried out using the Gaussian 03 program^[41] in the IBM P690 system at the Shandong Province High-Performance Computing Centre.

Acknowledgements

Financial support from the Natural Science Foundation of China (grant nos. 20325105, 20431010, 20571049, 20601017, 50673051), National Ministry of Science and Technology of China (grant no. 2001CB6105-07), and the Ministry of Education of China, Shandong University is gratefully acknowledged. We are also grateful to the Shandong Province High-Performance Computing Centre for a grant of computer time.

Keywords: density functional calculations · nanostructures · self-assembly · substituent effects

- [1] A. Hagfeldt, M. Grätzel, *Chem. Rev.* **1995**, *95*, 49–68.
- [2] M. C. Schlamp, X. Peng, A. P. Alivisatos, *J. Appl. Phys.* **1997**, *82*, 5837–5842.
- [3] H. Wohltjen, A. W. Snow, *Anal. Chem.* **1998**, *70*, 2856–2859.
- [4] M. Yun, N. V. Myung, R. P. Vasquez, C. Lee, E. Menke, R. M. Penner, *Nano Lett.* **2004**, *4*, 419–422.
- [5] H. Gan, H. Liu, Y. Li, Q. Zhao, Y. Li, S. Wang, T. Jiu, N. Wang, X. He, D. Yu, D. Zhu, *J. Am. Chem. Soc.* **2005**, *127*, 12452–12453.
- [6] A. D. Schwab, D. E. Smith, B. Bond-Watts, D. E. Johnston, J. Hone, A. T. Johnson, J. C. de Paula, W. F. Smith, *Nano Lett.* **2004**, *4*, 1261–1265.
- [7] X. Gong, T. Milic, C. Xu, J. D. Batteas, C. M. Drain, *J. Am. Chem. Soc.* **2002**, *124*, 14290–14291.
- [8] Z. Wang, C. J. Medforth, C. J. Shelnutt, *J. Am. Chem. Soc.* **2004**, *126*, 15954–15955.
- [9] B. A. Jones, M. J. Ahrens, M.-H. Yoon, A. Facchetti, T. J. Marks, M. R. Wasielewski, *Angew. Chem.* **2004**, *116*, 6523–6526; *Angew. Chem. Int. Ed.* **2004**, *43*, 6363–6366.
- [10] B. A. Gregg, R. A. Cormier, *J. Am. Chem. Soc.* **2001**, *123*, 7959–7960.
- [11] C. W. Struijk, A. B. Sieval, J. E. J. Dakhorst, M. van Dijk, P. Kimkes, R. B. M. Koehorst, H. Donker, T. J. Schaafsma, S. J. Picken, A. M. van de Craats, J. M. Warman, H. Zuihof, E. J. R. Sudholter, *J. Am. Chem. Soc.* **2000**, *122*, 11057–11066.
- [12] P. Ranke, I. Bleyl, J. Simmerer, D. Haarer, A. Bacher, H. W. Schmidt, *Appl. Phys. Lett.* **1997**, *71*, 1332–1334.
- [13] T. van der Boom, R. T. Hayes, Y. Zhao, P. J. Bushard, E. A. Weiss, M. R. Wasielewski, *J. Am. Chem. Soc.* **2002**, *124*, 9582–9590.
- [14] M. J. Fuller, L. E. Sinks, B. Rybtchinski, J. M. Giaimo, X. Li, M. R. Wasielewski, *J. Phys. Chem. A* **2005**, *109*, 970–975.
- [15] B. Rybtchinski, L. E. Sinks, M. R. Wasielewski, *J. Am. Chem. Soc.* **2004**, *126*, 12268–12269.
- [16] X. Li, L. E. Sinks, B. Rybtchinski, M. R. Wasielewski, *J. Am. Chem. Soc.* **2004**, *126*, 10810–10811.
- [17] F. Würthner, Z. Chen, V. Dehm, V. Stepanenko, *Chem. Commun.* **2006**, 1188–1190.
- [18] F. Würthner, *Pure Appl. Chem.* **2006**, *78*, 2341–2349.
- [19] F. Würthner, C. Thalacker, S. Diele, C. Tschierske, *Chem. Eur. J.* **2001**, *7*, 2245–2253.
- [20] Z. Chen, U. Baumeister, C. Tschierske, F. Würthner, *Chem. Eur. J.* **2007**, *13*, 450–465.
- [21] Z. Chen, V. Stepanenko, V. Dehm, P. Prins, L. D. A. Siebbeles, J. Seibt, P. Marquetand, V. Engel, F. Würthner, *Chem. Eur. J.* **2007**, *13*, 436–449.
- [22] C. Thalacker, F. Würthner, *Adv. Funct. Mater.* **2002**, *12*, 209–218.
- [23] L. E. Sinks, B. Rybtchinski, M. Iimura, B. A. Jones, A. J. Goshe, X. Zuo, D. M. Tiede, X. Li, M. R. Wasielewski, *Chem. Mater.* **2005**, *17*, 6295–6303.
- [24] A. Sautter, C. Thalacker, F. Würthner, *Angew. Chem.* **2001**, *113*, 4557–4560; *Angew. Chem. Int. Ed.* **2001**, *40*, 4425–4428.
- [25] K. Balakrishnan, A. Datar, R. Oitker, H. Chen, J. Zuo, L. Zang, *J. Am. Chem. Soc.* **2005**, *127*, 10496–10497.
- [26] K. Balakrishnan, A. Datar, T. Naddo, J. Huang, R. Oitker, M. Yen, J. Zhao, L. Zang, *J. Am. Chem. Soc.* **2006**, *128*, 7390–7398.
- [27] A. P. H. J. Schenning, J. V. Herrikhuysen, P. Jonkheijm, Z. Chen, F. Würthner, E. W. Meijer, *J. Am. Chem. Soc.* **2002**, *124*, 10252–10253.
- [28] E. H. A. Beckers, S. C. J. Meskers, A. P. H. J. Schenning, Z. Chen, F. Würthner, P. Marsal, D. Beljonne, J. Cornil, R. A. Janssen, *J. Am. Chem. Soc.* **2006**, *128*, 649–657.
- [29] E. H. A. Beckers, Z. Chen, S. C. J. Meskers, P. Jonkheijm, A. P. H. J. Schenning, X. Li, P. Osswald, F. Würthner, R. A. J. Janssen, *J. Phys. Chem. B* **2006**, *110*, 16967–16978.
- [30] F. Würthner, *Chem. Commun.* **2004**, 1564–1579.
- [31] D. Horn, J. Rieger, *Angew. Chem.* **2001**, *113*, 4460–4492; *Angew. Chem. Int. Ed.* **2001**, *40*, 4330–4361.
- [32] E. Rabinowitch, L. Epstein, *J. Am. Chem. Soc.* **1941**, *63*, 69–78.
- [33] W. West, S. Pearce, *J. Phys. Chem.* **1965**, *69*, 1894–1903.
- [34] X. Li, X. He, A. C. H. Ng, D. K. P. Ng, C. Wu, *Macromolecules* **2000**, *33*, 2119–2123.
- [35] F. Würthner, V. Stepanenko, Z. Chen, C. R. Saha-Möller, N. Kocher, D. Stalke, *J. Org. Chem.* **2004**, *69*, 7933–7939.
- [36] C. Zhao, Y. Zhang, R. Li, X. Li, J. Jiang, *J. Org. Chem.* **2007**, *72*, 2402–2410.
- [37] X. C. Gong, T. Milic, C. Xu, J. D. Batteas, C. M. Drain, *J. Am. Chem. Soc.* **2002**, *124*, 14290–14291.
- [38] B. K. An, S. K. Kwon, S. D. Jung, S. Y. Park, *J. Am. Chem. Soc.* **2002**, *124*, 14410–14415.
- [39] H. Matsuda, E. Van Keuren, A. Masaki, K. Yase, A. Mito, C. Takahashi, H. Kasai, H. Kamatani, S. Okada, H. Nakanishi, *Nonlinear Opt.* **1995**, *10*, 123–128.
- [40] C. Peng, P. Y. Ayala, H. B. Schlegel, M. J. Frisch, *J. Comput. Chem.* **1996**, *17*, 49–56.
- [41] M. J. Frisch, G. W. Trucks, H. B. Schlegel, G. E. Scuseria, M. A. Robb, J. R. Cheeseman, Jr., Montgomery, T. Vreven, K. N. Kudin, J. C. Burant, J. M. Millam, S. S. Iyengar, J. Tomasi, V. Barone, B. Mennucci, M. Cossi, G. Scalmani, N. Rega, G. A. Petersson, H. Nakatsuji, M. Hada, M. Ehara, K. Toyota, R. Fukuda, J. Hasegawa, M. Ishida, T. Nakajima, Y. Honda, O. Kitao, H. Nakai, M. Klene, X. Li, J. E. Knox, H. P. Hratchian, J. B. Cross, C. Adamo, J. Jaramillo, R. Gomperts, R. E. Stratmann, O. Yazyev, A. J. Austin, R. Cammi, C. Pomelli, J. W. Ochterski, P. Y. Ayala, K. Morokuma, G. A. Voth, P. Salvador, J. J. Dannenberg, V. G. Zakrzewski, S. Dapprich, A. D. Daniels, M. C. Strain, O. Farkas, D. K. Malick, A. D. Rabuck, K. Raghavachari, J. B. Foresman, J. V. Ortiz, Q. Cui, A. G. Baboul, S. Clifford, J. Cioslowski, B. B. Stefanov, G. Liu, A. Liashenko, P. Piskorz, I. Komaromi, R. L. Martin, D. J. Fox, T. Keith, M. A. Al-Laham, C. Y. Peng, A. Nanayakkara, M. Challacombe, P. M. W. Gill, B. Johnson, W. Chen, M. W. Wong, C. Gonzalez, J. A. Pople, Gaussian 03, Revision B.05; Gaussian, Inc., Pittsburgh, PA, **2003**.

Received: April 12, 2007

Published online on July 6, 2007